BAAA, Vol. 64, 2023
R.D. Rohrmann, C.H. Mandrini, C.E. Boeris & M.A. Sgró, eds.

Asociación Argentina de Astronomía
Boletín de artículos científicos

Mapping cosmic rays ionization on cores of molecular clouds and its effects on deuterium chemistry

G. Latrille[1], S. Bovino[1], A. Lupi[2], T. Grassi[3] & M. Padovani[4]

[1] *Departamento de Astronomía, Universidad de Concepción, Chile*
[2] *Department of Physics Giuseppe Occhialini, University of Milano-Bicocca, Italia*
[3] *Centre for Astrochemical Studies, Max-Planck-Institut für extraterrestrische Physik, Alemania*
[4] *Istituto Nazionale di Astrofisica, Osservatorio Astrofisico di Arcetri, Italia*

Contact / gonzajaque2016@udec.cl

Resumen / Presentamos los resultados de un nuevo código numérico que simula la propagación de los rayos cósmicos dentro de nubes moleculares. Empleamos el código para obtener mapas de la tasa de ionización por rayos cósmicos en simulaciones magnetohidrodinámicas 3d de núcleos preestelares. El mapa es luego usado para seguir la subsecuente evolución química de especies deuteradas incluida en nuestro marco de post-procesamiento. El análisis de especies deuteradas muestra un incremento de trazadores cruciales con respecto al mismo análisis realizado con una tasa de ionización por rayos cósmicos fija a un valor constante. Esto tiene consecuencias importantes en el tiempo que le toma a los procesos de deuteración y su utilidad como relojes químicos en las regiones de formación estelar.

Abstract / We present the results of a new numerical code which simulates cosmic rays propagation within molecular clouds. We employ the code to obtain cosmic ray ionization rate maps of 3d magneto-hydrodynamic simulations of prestellar cores. The maps are then used to follow the subsequent chemical evolution of deuterated-species within our post-processing framework. The analysis of deuterated-species shows an increasing of key tracers with relative to the same analysis performed on a run with the cosmic ray ionization rate set to a constant value. This has important consequences for the overall timescale of the deuteration process and its usefulness as a chemical clock in star-forming regions.

Keywords / ISM: clouds — cosmic rays — ISM: molecules

1. Introduction

Dense cores (sizes of 0.05 - 0.1 pc) inside molecular clouds are the birthplace of stars, and are characterized by low temperatures ($T < 20$ K) and high densities ($n > 10^4$ cm^{-3}). Due to the low temperature, several molecular species besides CO, such as methane (CH_4), methanol (CH_3OH) and water (H_2O), are adsorbed on the surface of dust-grains in the form of ices (van Dishoeck, 2014).

In addition, due to the high density in the envelope surrounding these cores, radiation cannot penetrate, and the only source of ionization are cosmic rays (hereafeter CRs). CRs are highly energetic particles (energies from 100 eV up to 10^{21} eV), where protons, He nucleus and carbon amount to 98%, and the rest is in positrons and electrons. As they are the only type of radiation that can penetrate the layers of dense cloud, they are responsible for triggering ion-molecule reactions (Watson, 1974; Padovani et al., 2009). The first step of this process is the ionization of molecular hydrogen and the subsequent reaction to produce H_3^+, the main molecular ion in these regions. The presence of CRs in such environments results in the proliferation of several species through isotopic fractionation of H_3^+ (Watson, 1974; Caselli et al., 2019).

Deuterated molecules are the main tools to know the state of dense cores (Caselli et al., 2019), since H_3^+ can easily react with HD to produce H_2D^+, starting the deuterium fractionation (deuteration) process which also produces, for instance, DCO^+ and N_2D^+ (Caselli et al., 2019; Indriolo & McCall, 2013). Among the different deuterated tracers, o-H_2D^+ and DCO^+ are also employed as proxies of the cosmic ray ionization rate (ζ_2, hereafter CRIR), i.e. the number of H_2 molecules ionized per unit time (Caselli et al., 1998; Bovino et al., 2020).

In this study, we focus on the impact of properly modelling the propagation of CRs through magnetised dense cores to then study the evolution of deuterated species like o-H_2D^+ and DCO^+. We compare the results obtained with the propagation scheme (which depends on the effective column density $N_{\rm eff}$, being the column density traversed by CRs, which path may differ from the usual line-of-sight according to how magnetic fields are twisted) to those obtained in the original simulation employing a standard constant value of the CRIR ζ_c.

2. Methodology

For the following analysis, we use the collapsing core presented in Bovino et al. (2019). The simulations have been performed with the magneto-hydrodynamic code GIZMO (Hopkins, 2015; Hopkins & Raives, 2016) coupled

Poster contribution

with the thermochemistry package KROME (Grassi et al., 2014).

Our reference simulation assigns to each particle from the cloud the same constant value of $\zeta_c = 2.5 \times 10^{-17}$ s^{-1}. We compare this reference simulation with a propagation scheme of cosmic rays based on tracer particles (TPs), which is applied in post-processing. In this work, cosmic rays are sampled with a total of 10240 TPs, which are injected in the cloud at 0.5 pc from the cloud center. Their propagation is then followed by taking into account their coupling to the magnetic field lines. During their journey, TPs keep track of the effectively traversed gas column density $N_{\rm eff}$, which is used to consistently update ζ_2. The propagation for each TP is computed by means of a Runge-Kutta integrator, with the step defined by the smoothing length h_i at the current location of the TP obtained using a spline kernel encompassing 32 gas neighbours from the original simulation. At each step, a new value of ζ_2 for each TP is determined, by appropriately weighting each gas particle contribution to the kernel volume. It is worth notice that, as TPs move deep into the core, the cosmic ray ionization rate continuously decreases as a function of the effective column density $N_{\rm eff}$.

At the end of the calculations, A CRIR map is generated for each snapshot of the original simulation, and it is then passed as an input to the post-processing code developed and presented by Ferrada-Chamorro et al. (2021), using the same initial conditions and networks employed by Bovino et al. (2019). The chemical evolution of the core is performed via KROME (Grassi et al., 2014) according to the density and temperature from the simulated snapshots and CRIR map provided from the propagator.

3. Results

In Fig. 1, we report the density-weighted map of the CRIR, obtained from the propagation code at 153.3 kyr. The map shows a highly ionized core, with the ionization rate decreasing towards the center. This high ionization rate is due to the initial injected CRIR ($\sim 3 \times 10^{-16}$ s^{-1}). The high-ionization initial value comes from the theoretical model $\mathscr{H}$ presented by Padovani et al. (2022), which aims to mimic the CRIR observational estimates obtained for diffuse cloud. The decrease is in line with theoretical prediction, in which CRs that penetrate deeper into the cloud have to traverse higher column densities, and are attenuated. In Fig. 2, we show column density maps for specific tracers (o-H_2D^+ and DCO^+) at 153.3 kyr obtained from our post-processing framework, using the computed CRIR maps. Left panels correspond to the reference run with constant CRIR, while the right ones show the case where CRs have been propagated. We notice an increase of column density for both tracers when a proper CRs propagation is considered. DCO^+ is boosted up to a factor of seven compared to the constant CRIR case, while o-H_2D^+ presents an overabundance of a factor of three. In Fig. 3, we also show the radial profiles for the two tracers. Spatially, the radial profile of o-H_2D^+ follows the case with constant CRIR. The same happens for DCO^+. On the other hand, the impact of the CRIR produces a considerable enhancement of DCO^+ formation.

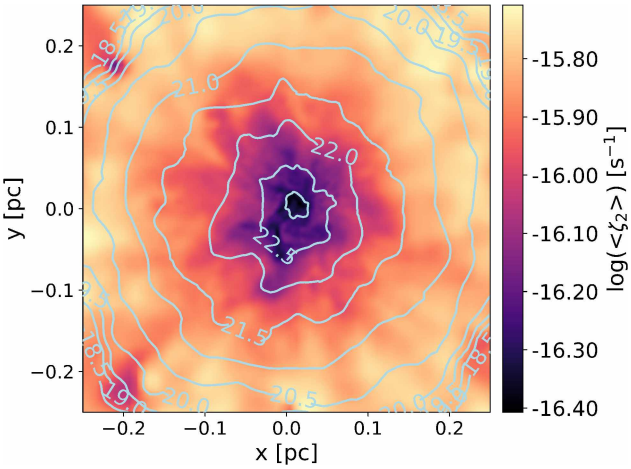

Figure 1: Cosmic ray ionization rate map density-weighted produced by our propagator at 153.3 kyr within 0.2 pc as depth length. Contours show total column density N.

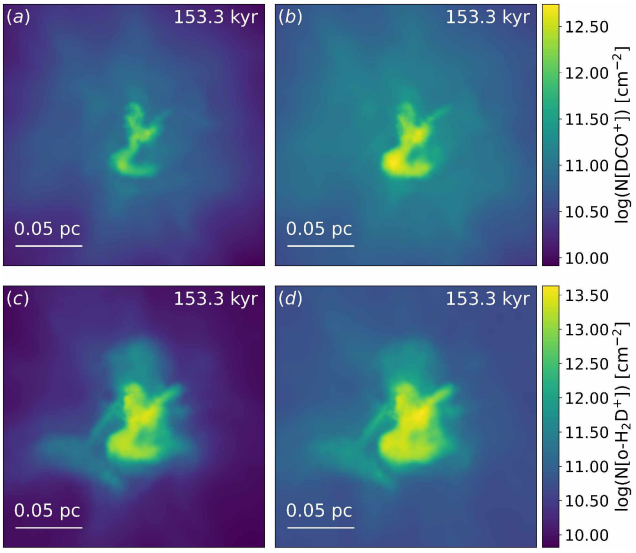

Figure 2: Column density maps within 0.2 pc as depth length for DCO^+ and o-H_2D^+ obtained from our simulations. Panel (a) and (c) show the column density maps of both species for the simulations with a constant CRIR. (b) and (d) show the same but for the model given by our propagator.

4. Conclusion

In this work, we presented the first self-consistent simulations of collapsing dense cores where chemistry and cosmic-ray propagation have been accurately treated. The results show a decrease of the CRIR towards the center of the core due to the increase of the column density. CRs are injected outside the core and propagate along the magnetic field lines. The impact of the CRIR on deuterated species such as DCO^+ is significant.

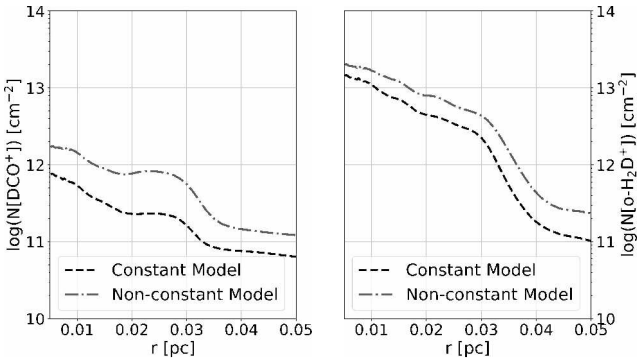

Figure 3: Column density radial profiles for DCO^+ (*left*) and o-H_2D^+ (*right*) for the two simulations performed in this work. The blue dashed lines correspond to our propagation scheme, and the black solid lines to the original simulation. The column densities are calculated by assuming a core depth of 0.05 pc.

These first runs provided a useful testbed for our CRs propagator and the impact on the chemistry of deuterated species. In future works, we will study the impact of CRIR on a wide range of tracers and the overall effect on key processes like deuterium fractionation, which can have relevant consequences for the use of chemical clocks in star-forming regions.

Acknowledgements: SB is financially supported by Fondecyt Regular (project 1220033). AL acknowledges funding from MIUR under the grant PRIN 2017-MB8AEZ.

References

Bovino S., et al., 2019, ApJ, 887, 224
Bovino S., et al., 2020, MNRAS, 495, L7
Caselli P., Sipilä O., Harju J., 2019, Philos. Trans. R. Soc., 377, 20180401
Caselli P., et al., 1998, ApJ, 499, 234
Ferrada-Chamorro S., Lupi A., Bovino S., 2021, MNRAS, 505, 3442
Grassi T., et al., 2014, MNRAS, 439, 2386
Hopkins P., 2015, MNRAS, 450, 53
Hopkins P.F., Raives M.J., 2016, MNRAS, 455, 51
Indriolo N., McCall B.J., 2013, Chem. Soc. Rev., 42, 7763
Padovani M., Galli D., Glassgold A.E., 2009, A&A, 501, 619
Padovani M., et al., 2022, A&A, 658, A189
van Dishoeck E.F., 2014, Faraday Discuss., 168, 9
Watson D.W., 1974, ApJ, 188, 35